Phase Equilibria and Modeling of Ammonium Ionic Liquid, C_2NTf_2, Solutions†

Urszula Domańska,* Andrzej Marciniak, and Marek Królikowski

Physical Chemistry Division, Faculty of Chemistry, Warsaw University of Technology, Noakowskiego 3, 00-664 Warsaw, Poland

Received: August 18, 2007; In Final Form: October 17, 2007

Novel quaternary ammonium ionic liquid, ethyl(2-hydroxyethyl)dimethylammonium bis(trifluomethylsulfonyl)-imide (C_2NTf_2), has been prepared from *N*,*N*-dimethylethanolamine as a substrate. The paper includes a specific basic characterization of the synthesized compound by NMR and the basic thermophysical properties: the melting point, enthalpy of fusion, enthalpy of solid−solid phase transition, glass transition determined by the differential scanning calorimetry (DSC), temperature of decomposition, and water content. The density of the new compound was measured. The solid−liquid or liquid−liquid phase equilibria of binary mixtures containing {C_2NTf_2 + water or an alcohol (propan-1-ol, butan-1-ol, hexan-1-ol, octan-1-ol, decan-1-ol), aromatic hydrocarbons (benzene, toluene), aliphatic hydrocarbons (*n*-hexane, *n*-octane), dimethylsulfoxide (DMSO), or tetrahydrofuran (THF)} have been measured by a dynamic method in a wide range of temperatures from 230 to 430 K. These data were correlated by means of the nonrandom two-liquid (NRTL) equation utilizing temperature-dependent parameters derived from the solid−liquid or liquid−liquid equilibrium. From the solubility results, the negative value of the partition coefficient of ionic liquid in binary system octan-1-ol/water (log *P*) at 298.15 K has been calculated.

Introduction

Quaternary ammonium salts (quats) are widely used for many applications, such as lubricating materials, cationic surfactants, fabric softeners, ant electrostatics, adhesion promoters in asphalt, corrosion inhibitors, and many others.[1−5] Recently, new applications for quat-based ammonium ionic liquids (ILs), derived from common, ammonium-based cations with a nitrate anion, have been presented.[6−8] These salts are useful as anti-bacterial, anti-fungal agents and wood preservatives. The phase equilibrium of two salts, (benzyl)dimethylalkylammonium and didecyldimethylammonium nitrates with water, aromatic and aliphatic hydrocarbons, and alcohols have been described.[7,8] The toxicity of these ILs were also studied.[6] Alkyl(2-hydroxyethyl)-dimethylammonium bromides as precursors of ILs have been prepared.[9−11] Thermodynamic properties and the partition coefficients in octan-1-ol/water binary system of these bromides[9] and the solubilities in alcohols[10] were described. The solid−liquid equilibrium (SLE) and liquid−liquid equilibrium (LLE) of ethyl(2-hydroxyethyl)dimethylammonium tetrafluoroborate (C_2BF_4), ethyl(2-hydroxyethyl)dimethylammonium hexafluorophosphate (C_2PF_6), or ethyl(2-hydroxyethyl)dimethylammonium dicyanamide ($C_2N(CN)_2$) with water or chosen alcohols have been presented.[11] Most of these binary systems were described as a simple eutectic system with or without immiscibility in the liquid phase with the upper critical solution temperature (UCST). The solubility of alkyl(2-hydroxyethyl)-dimethylammonium bromides in polar solvents such as water and alcohol increases with an increase of the alkyl chain length from C_2 to C_6 of substituent on the nitrogen atom. This could possibility be explained as a result of the intermolecular hydrogen bonding between salt and solvent. However, the enhancement in solubility with increased alkyl chain length was explained by the lower melting temperature of the salt and increased ability of longer alkyl chain of the cation to interact with the alkyl portion of the alcohol via van der Waals interaction. The octan-1-ol/water partition coefficients, log *P* for these salts, are negative.[9] The solubility in alcohols is typical for every kind of ionic liquid as imidazolium, phosphonium, or ammonium: in general, (IL + an alcohol) binary mixtures show LLE with UCST shifted to the alcohol higher mole fraction. An increase in the alkyl chain length of the alcohol resulted in an increase of the UCST.[10] For different anions such as tetrafluoroborate, hexafluorophosphate, or dicyanamide and ethyl(2-hydroxyethyl)dimethylammonium cation, the melting temperature of the IL salts are much lower than those of the bromide salts. The SLE for C_2BF_4 with hydrocarbons, hexane, heptane, and cyclohexane, presented typical dependencies. Usually, the UCST increases as the length of the alkyl chain of the hydrocarbon increases, and in cyclohexane, solubility decreases in comparison with *n*-alkanes (the UCST increases).[11]

New chiral ammonium-based ILs containing the (1*R*,2*S*,5*R*)-(−)-menthyl group have been synthesized.[12] These salts have been demonstrated to be air- and moisture-stable under ambient conditions and have also been found to exhibit strong antimicrobial and high ant electrostatic activities.[12]

A number of excellent reviews are already available where the properties and applications of ILs have been described.[13−16] Ionic liquids can be used to enhance the efficiency of a wide range of electrochemical, analytical, synthetic, and engineering processes.

It has been proved that the nonrandom two-liquid (NRTL) model works very well in modeling activity coefficients of quaternary ammonium ILs in alcohols[9,10] and electrolyte NRTL model in water.[17]

This work includes synthesis, physicochemical properties and the phase equilibria measurements of quaternary ammonium salt ethyl(2-hydroxyethyl)dimethylammonium bis(trifluoromethyl-

* To whom correspondence should be addressed. E-mail: ula@ch.pw.edu.pl.

† Presented at the 2nd International Congress on Ionic Liquids (COIL2), Yokohama, Japan, August 5−10, 2007.

10.1021/jp076652s CCC: $40.75
Published on Web 01/08/2008

TABLE 1: Thermophysical Constants of Pure Salt, Determined from DSC Data

compound	$T_{fus,1}$/K	$\Delta_{fus}H_1$/kJ·mol^{-1}	$T_{tr,1}$/K	$\Delta_{tr}H_{1,1}$/kJ·mol^{-1}	$T_{tr,11}$/K	$\Delta_{tr}H_{1,11}$/kJ·mol^{-1}	T_{dec}/K
C_2 NTf_2	279.16	2.83	262.5	0.84	232.8; 180(g)[a]	10.02	700[b]

[a] Glass transition (g). ΔCp at the glass transition is equal to 50.2 J·mol^{-1}·K^{-1}. [b] Mass loss 20%.

TABLE 2: Solid−Liquid Equilibria (SLE) and Liquid−Liquid Equilibria (LLE) of the Binary System {C_2NTf_2 + Water}

x_1	T_1^{SLE}/K	T_1^{LLE}/K	x_1	T_1^{SLE}/K	T_1^{LLE}/K
1.0000	279.16		0.4282	251.55	312.63
0.9510	277.36		0.3951	251.55	318.98
0.9294	275.39		0.3503	251.55	326.28
0.8492	268.06		0.3075	251.55	331.46
0.8021	263.50		0.2651	251.55	338.26
0.7529	259.37		0.2287	251.55	345.08
0.7108	256.18		0.1994	251.55	351.36
0.6665	252.73		0.1616	251.55	359.70
0.6253	251.50		0.1169	251.55	368.35
0.5865	251.48	278.50	0.0791	251.55	
0.5539	251.55	287.81	0.0114		359.52
0.5221	251.55	294.40	0.0053		331.46
0.4711	251.55	304.74	0.0000	273.15	

sulfonyl)imide, C_2NTf_2 with water, alcohols, aromatic hydrocarbons, aliphatic hydrocarbons, dimethylsulfoxide (DMSO), or tetrahydrofuran (THF). This paper is a continuation of our wide ranging of investigation into quaternary ammonium salts. It is worth noting that the IL under investigation here is a liquid at room temperature.

Experimental Procedures and Results

Materials. Investigated compound was prepared using the *N*,*N*-dimethylethanolamine (Sigma-Aldrich CAS number 108-01-0) and ethyl bromide (Sigma-Aldrich CAS number 74−96-4). The reagents were mixed in 10% excess of haloalkane. The intermediates were heated at 80 °C for 30 min and stirred under reflux to form the reaction mixture. After that, the mixture was cooled down, and the obtained solid product was dissolved in mixture of propan-1-ol (Sigma-Aldrich CAS number 71-23-8) and methanol (Sigma-Aldrich CAS number 67-56-1) at ratio 1:3. Subsequently, the mixture was heated at 80 °C for 30 min under reflux. Later, the mixture was cooled down, and a very small portion of cyclohexane (Sigma-Aldrich CAS number 110-82-7) was added into the mixture to form the solid powder. The solid phase was filtered through the S4 filter, and that phase was collected. The salt was recrystallized from the mixture of propan-1-ol and methanol and then rigorously dried under vacuum for 48 h prior to use as was described previously.[9] The second step of the synthesis involved metathesis of the bromide with the lithium salt of bis(trifluoromethanesulfonyl)imide, Li-[NTf_2]. The ion-exchange reaction proceeded efficiently in distilled water, with yields higher than 85−99%.

The compound was characterized using ^{1}H NMR, DSC, TG/DTA, and water content. The brief characterization of the obtained compound is presented in Table 1 and as GRS 1−3 of Supporting Information.

All solvents were obtained from Sigma-Aldrich Chemie GmbH, Steinheim, Germany, and were fractionally distilled to a mass percent purity better than 99.8. Solvents were stored over freshly activated molecular sieves of type 4A (Union Carbide). Twice distilled and degassed water was used for the solubility measurements.

Nuclear Magnetic Resonance (NMR). ^{1}H NMR spectra in $CDCl_3$ solutions was recorded on Varian Gemini 2000 spectrometer. Description of spectra is presented as GRS 1.

Differential Scanning Microcalorimetry (DSC). The melting point, the enthalpy of fusion, and the enthalpy of the solid−solid phase transition of quaternary ammonium salt was measured using a differential scanning microcalorimetry (DSC) at the 5 K·min^{-1} scan rate with the power sensitivity of 16 mJ·s^{-1} and with the recorder sensitivity of 5 mV. The instrument (Perkin Elmer Pyris 1) was calibrated before each measurement with the 99.9999 mol % purity indium sample. The calorimetric accuracy was ±1%, and the calorimetric precision was ±0.5%. The thermophysical properties are shown in Table 1 and GRS 2 of Supporting Information.

Decomposition of Compound. Simultaneous TG/DTA experiments were performed using a MOM Derivatograph−PC (Hungary). In general, runs were carried out using matched labyrinth platinic crucibles with Al_2O_3 in the reference pan. The crucible design hampered the migration of volatile decomposition products reducing the rate of gas evolution and, in turn, increasing contact time of the reactants. The TG/DTA curve was obtained at 5 K·min^{-1} heating rate with a nitrogen dynamic atmosphere (flow rate 20 dm^3·h^{-1}). The temperatures of decomposition and percents of mass loss are presented in GRS 3.

Water Content. The water content was analyzed by Karl−Fischer titration technique (method TitroLine KF). The sample of IL was dissolved in methanol and titrated with steps of 2.5 μL. The results obtained have shown the water content to be less than 200 ppm.

Solid−Liquid/Liquid−Liquid Phase Equilibria Apparatus and Measurements. Solid solubilities or the two phases disappearance observed with an increasing temperature have been determined using a dynamic (synthetic) method described previously.[7−11] The compound was kept under the nitrogen in a drybox. Mixtures of solute and solvent were prepared by weighing the pure components to within 1×10^{-4} g. The sample of solute and solvent was heated very slowly (at less than 2 K·h^{-1} near the equilibrium temperature) with continuous stirring inside a Pyrex glass cell, placed in a thermostat (see the schematic diagram of the method in Figure 1S of Supporting Information). The crystal disappearance temperatures or foggy solution disappearance detected visually were measured with a calibrated Gallenkamp Autotherm II thermometer. The measurements were carried out over a wide range of solute mole fraction ranging from 0 to 1. The uncertainty of temperature measurements was ±0.05 K, and that of the mole fraction did not exceed ±0.0005. The reproducibility of the SLE/LLE experimental points was ±0.1 K. The experimental results are listed in Table 2 and Table 1S of Supporting Information.

Density Measurements. The density of IL was measured using an Anton Paar DMA 602 vibrating-tube densimeter thermostated at $T = (298.15 \pm 0.01)$ K. The densimeter's calibration was performed at atmospheric pressure using doubly distilled and degassed water, specially purified benzene (CHEMIPAN, Poland 0.999), and dried air. The vibrating−tube temperature was measured by an Anton Paar DM 100−30 digital thermometer and was regulated to within better than ±0.01 K using a UNIPAN 60 thermostat and 202 temperature control system (UNIPAN, Poland). The error in density being estimated as lower than 5×10^{-5} g·cm^{-3}. The density of IL is shown in Table 2S of Supporting Information.

Results

Ethyl(2-hydroxyethyl)dimethylammonium bromide was prepared by treating the *N*,*N*-dimethylethanolamine with ethyl bromide as was described previously.[9] The NMR analysis shows no unexpected signals, that is, unremoved solvents or unreacted intermediates. The IL is a colorless liquid, nonflammable, and partly miscible with water, alcohols, and many organic solvents. Karl−Fischer measurement showed that the water content of the dried salt to be less than 200 ppm. The DSC diagram (see GRS 2 of Supporting Information and Table 1) gives the melting point at 279.16 K, with a low heat of fusion $\Delta_{fus}H_1 = 2.83$ kJ·mol^{-1} and the characteristic two solid−solid phase transitions at 262.5 and 232.8 K with corresponding heats of phase transition equal to 0.84 and 10.02 kJ·mol^{-1}. The enthalpies of two solid−solid phase transitions diminish the enthalpy of melting of C_2NTf_2. It can be seen also, that the melting peak is divided into two parts, which means that after a few heating runs performed on the same sample, the new solid−solid phase transition at the temperature close to the melting point can be expected. It is worth noting that a similar salt with a different anion, $[Br]^-$, has revealed only one solid−solid phase transition.[9] The glass transition temperature of C_2NTf_2 was 180 K. The glass transition temperatures for the similar ILs as alkyl(2-hydroxyethyl)dimethylammonium bromides were close to this temperature and were as follows: 216, 166, 187, and 184 K for ethyl-, propyl-, butyl-, and hexyl- substituents, respectively.[9] For IL with more polar anion as for ethyl(2-hydroxyethyl)-dimethylammonium dicyanamide, the glass temperature was 168 K.[11]

The salt obtained has a very high decomposition temperature of 700 K, determined from onset to 20% mass loss. For the C_2Br salt, it was at a lower temperature, about 530 K with 20% mass loss.[9]

In this work, the solid−liquid phase equilibria (SLE) and liquid−liquid phase equilibria (LLE) for a number of binary ionic liquid−water or organic solvent systems were determined. Table 2 includes direct experimental results of the SLE equilibrium temperatures, T^{SLE} and of the LLE equilibrium temperatures, T^{LLE} versus ionic liquid mole fraction, x_1, for the system {C_2NTf_2 + water}. Complete miscibility at the IL mole fraction higher than 0.57 was observed. Figure 1 shows the SLE/LLE diagram with the upper critical solution temperature (UCST). The maximum of the binodal curve was greater than 370 K and was at a low IL mole fraction. The left-hand limits of the equilibrium curves in this system and many others[18−23] are very close to zero mole fraction of IL, that is, $x_1 \approx 10^{-4}$. The eutectic point of the system was not observed as it was below 250 K and was very close the mole fraction of water, being equal to one. Water, an associating polar solvent, can interact with the anion $[NTf_2]^-$ of the salt and with the hydroxyl group of the cation. In spite of it, the interaction between four alkyl substituents at the cation and water and probably the improper packing effects in the liquid phase results in an immiscibility in the liquid phase. For the C_2Br and C_2BF_4 salts, simple eutectic systems were observed with complete miscibility in the liquid phase.[9,11] Similar results to be presented in this work were published for (benzyl)dimethylalkylammonium nitrate ([BA][NO_3]) with water,[7] but complete miscibility in the liquid phase was observed for the salt with the different cation, didecyldimethylammonium nitrate ([DDA][NO_3]).[8]

The systematic studies of the impact of different factors on the phase behavior of imidazolium based ionic liquids with alcohols was presented by many authors.[18−29] An increase in the alkyl chain length of the alcohol resulted in an decrease of solubility. Branching of the alcohol results in a higher solubility of the alcohol in the ionic liquid. By increasing the alkyl chain length on the cation of IL, the UCST decreased. Replacement of the hydrogen at the C2 position of the imidazolium ring with a methyl group resulted in an decrease of solubility.[27,28]

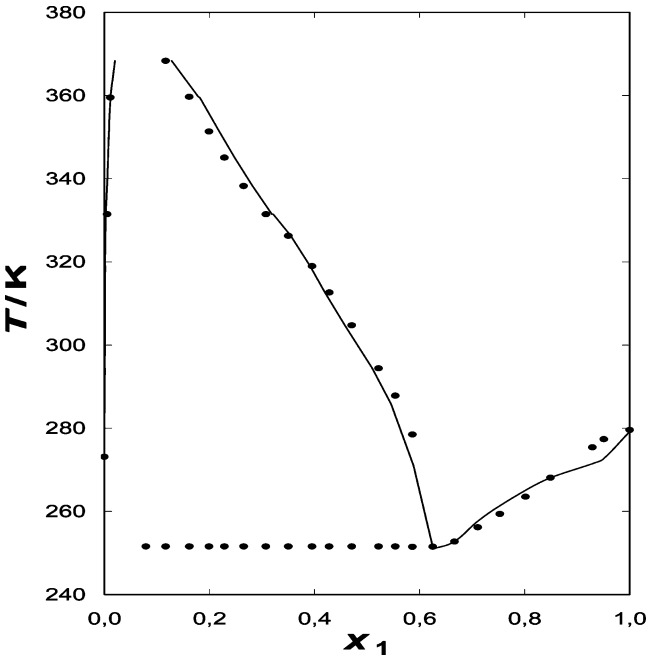

Figure 1. Solid−liquid and liquid−liquid phase equilibria of {C_2NTf_2 (1) + water (2)} binary system: points, experimental results; solid lines are calculated by means of the NRTL equation.

The effect of chemical and structural factors on the phase behavior of pyridinium ILs[30] was found to be the same as for imidazolium ILs.

Recently, the solubility of quaternary phosphonium salt, tetrabutylphosphonium methanesulfonate, {[($CH_3CH_2CH_2CH_2$)$_4$P][CH_3SO_3] + butan-1-ol, hexan-1-ol, octan-1-ol, decan-1-ol, or dodecan-1-ol} was presented.[31] Generally, the trend observed in the solubility changes of a phosphonium salt with respect to the alkyl chain length and benzene substitution of solvents is the same as was observed previously for ammonium salts. The increase of the alkyl chain of an alcohol decreases the solubility of IL.

The effect of interaction of ammonium salts with alcohols is different for different anions, for example, for C_2Br and C_2BF_4. The solubility of C_2Br ammonium salt in alcohols from ethanol to dodecan-1-ol did not present a miscibility gap,[9] while C_2BF_4 ammonium salt showed an immiscibility in the alcohols at high temperatures. These systems exhibited an UCST greater than 435 K.[11]

The solubility of C_2Br ammonium salt in primary alcohols (C_2−C_{12}) decreases with an increase of the alkyl chain of an alcohol.[10] The differences in solubilities between the primary and the secondary alcohols were not significant. It was observed that the solubility of C_2Br ammonium salt in ethanol was higher than the ideal solubility. This strong interaction with the solvent was explained by the similarity of an ethyl group connected with an OH group on the cation and the same length of alkyl chain of ethanol.

In this work, the complete miscibility in the liquid phase was observed in methanol and ethanol. In propan-1-ol, a small immiscibility gap was observed at very low temperatures (about 230−235 K). The SLE/LLE diagram is presented in Figure 2. In this system, the characteristic inflection on the liquidus curve

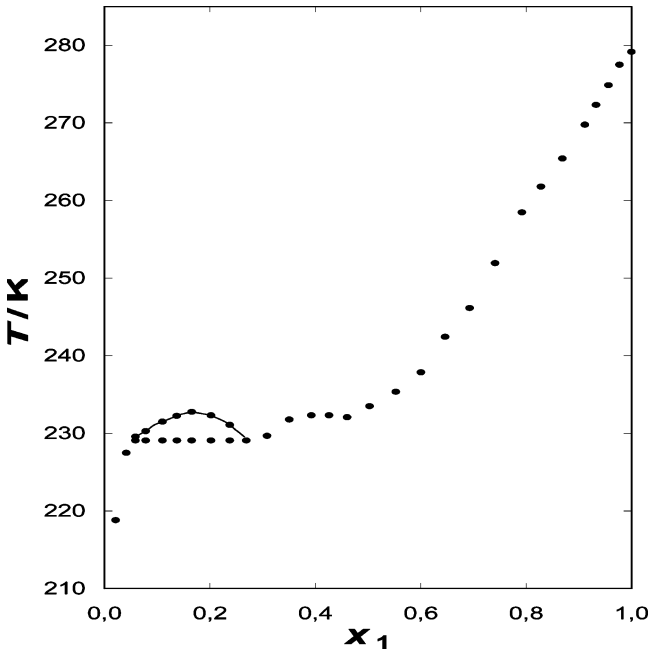

Figure 2. Solid−liquid and liquid−liquid phase equilibria of {C_2NTf_2 (1) + propan-1-ol (2)} binary system: points, experimental results; solid line for LLE is calculated by means of the NRTL equation.

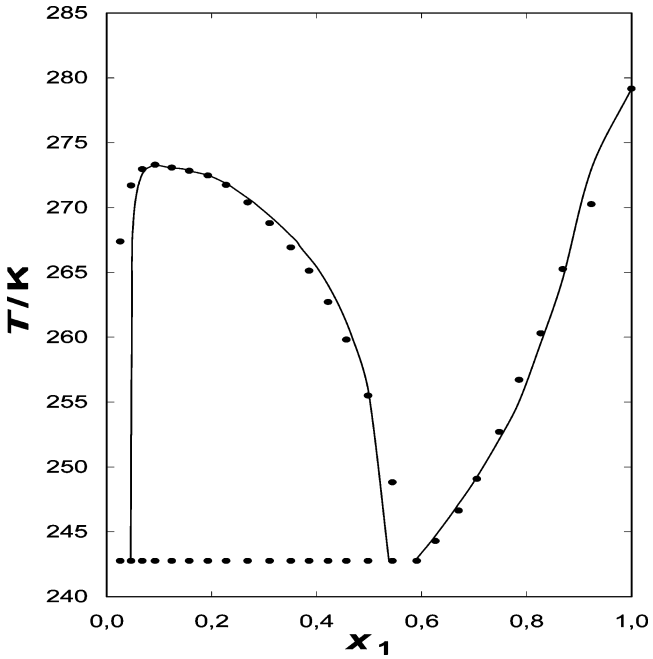

Figure 3. Solid−liquid and liquid−liquid phase equilibria of {C_2NTf_2 (1) + butan-1-ol (2)} binary system: points, experimental results; solid lines are calculated by means of the NRTL equation.

was observed at temperature 232.8 K, which is the effect of the solid−solid phase transition of C_2NTf_2 at this temperature. This is typical for molecular substances and ILs.[9−11,31] Experimental equilibrium temperatures for the systems {C_2NTf_2 + butan-1-ol, hexan-1-ol, octan-1-ol, decan-1-ol} are shown in Table 2S of Supporting Information.

In polar solvents, such as alcohols, one can expect stronger interaction between unlike molecules as an alcohol and the IL. Clearly, hydrogen bonding between hydroxyl group of an alcohol and that of cation or oxygen atoms of the anion plays an important role in controlling solid−liquid and liquid−liquid phase behavior of the investigated ammonium salt. However, the existence of the liquid−liquid phase equilibria in these mixtures is the evidence that the interaction between the IL and the solvent is not significant.

The solubility of C_2NTf_2 in alcohols decreases with an increase of the alkyl chain length of an alcohol. The UCSTs are 273.3, 218.3, and 364.3 K for the butan-1-ol, hexan-1-ol, and octan-1-ol, respectively. In the system {C_2NTf_2 + decan-1-ol}, the miscibility gap was observed over almost the whole range of IL mole fraction, and the UCST was above 430 K. The phase diagrams are presented in Figures 3−6 and all together in Figure 2S of Supporting Information. The experimental results are listed in Table 1S of Supporting Information.

Changing the solvent from an alcohol to an aromatic hydrocarbon demonstrates that the interaction is most likely due to $n-\pi$ interactions between the oxygen atoms of the IL (from the hydroxyl group of the cation or from the sulfonyl group of the anion) and the benzene ring contrary to hydrogen bonding.[7,8,32−34] The liquid−liquid equilibria for binary mixtures of {C_2NTf_2 + benzene, or toluene} is presented in Figure 7. Replacing the decan-1-ol by benzene significantly increases the solubility at any particular temperature. The miscibility gap in benzene is higher than that observed in butan-1-ol. For {C_2NTf_2 + toluene} binary system, the solubility in the liquid phase decreases. The UCSTs of these mixtures were not detected experimentally because they were above 430 K. For these two solvents, benzene had the lower UCST; this indicates the influence of an increased interaction of the IL with solvent. The

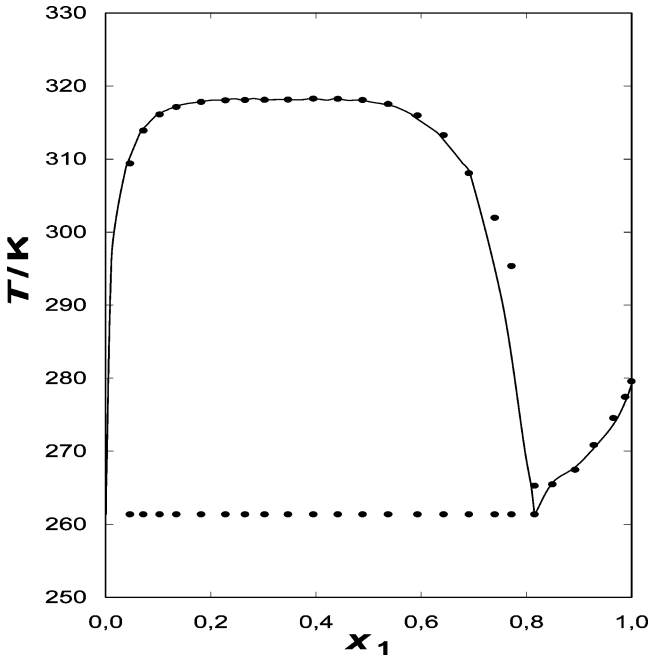

Figure 4. Solid−liquid and liquid−liquid phase equilibria of {C_2NTf_2 (1) + hexan-1-ol (2)} binary system: points, experimental results; solid lines are calculated by means of the NRTL equation.

same results were observed for imidazolium and phosphonium salts.[31−34] As usual, the lengthening of the aliphatic chain at the cation results in the same effects of interaction with solvent and/or has the same influence on packing effects. The phase diagram of {C_2NTf_2 + benzene} was complete, and the eutectic point was found graphically: $x_{1,e} = 0.677$ at $T_{1,e} = 237$ K. Table 1S lists temperature and composition of the saturated solutions for the investigated mixture. The eutectic point in the binary mixture of {C_2NTf_2 + toluene} is expected at a very low temperature of 230 K and low toluene mole fraction.

Similar effects were observed in the liquid−liquid equilibrium measurements in the system {C_2NTf_2 + *n*-hexane or *n*-octane}. The numerical data are presented in Table 1S of Supporting

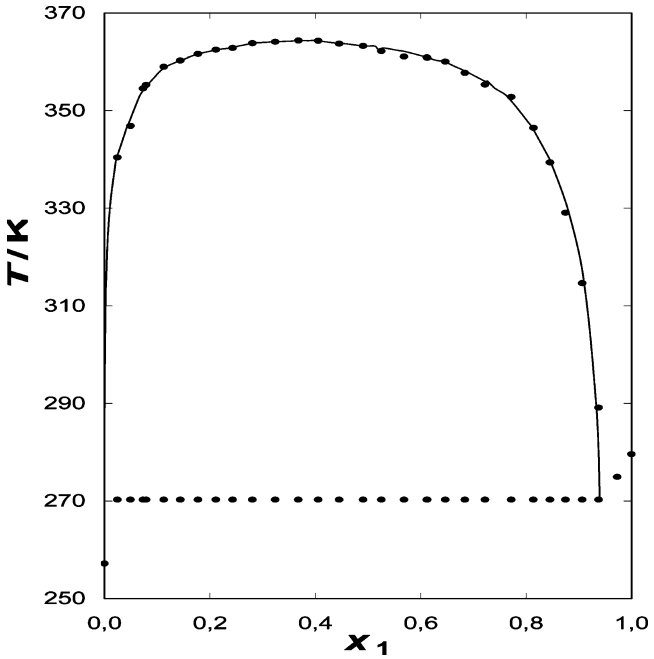

Figure 5. Solid−liquid and liquid−liquid phase equilibria of {C_2NTf_2 (1) + octan-1-ol (2)} binary system: points, experimental results; solid line for LLE is calculated by means of the NRTL equation.

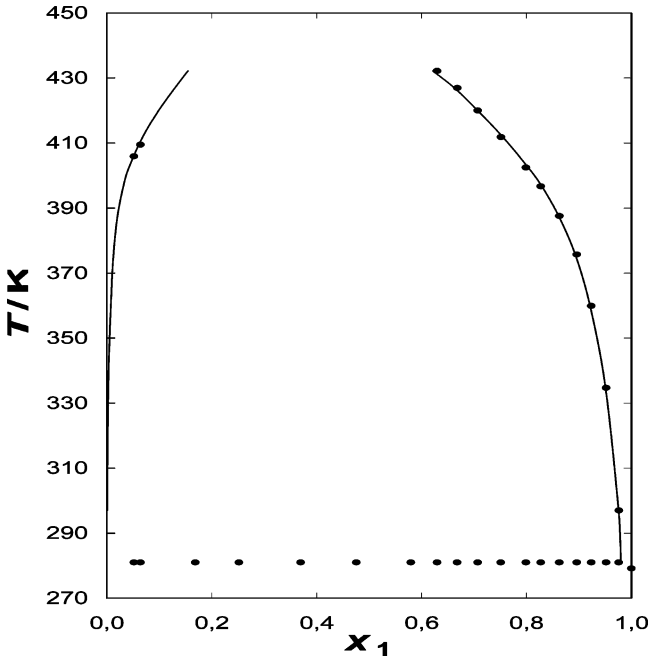

Figure 6. Solid−liquid and liquid−liquid phase equilibria of {C_2NTf_2 (1) + decan-1-ol (2)} binary system: points, experimental results; solid line for LLE is calculated by means of the NRTL equation.

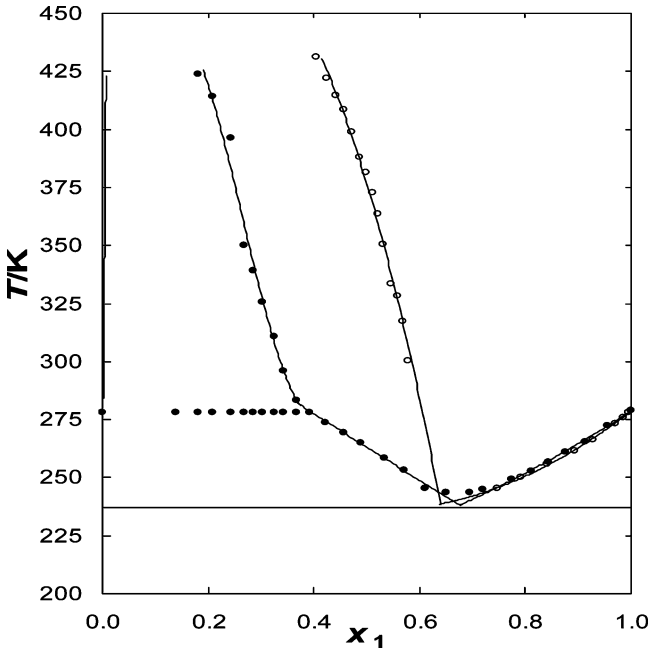

Figure 7. Solid−liquid and liquid−liquid phase equilibria of {C_2NTf_2 (1) + benzene, or toluene (2)} binary systems: (●) benzene; (○) toluene. Solid line for LLE and SLE (toluene) is calculated by means of the NRTL equation.

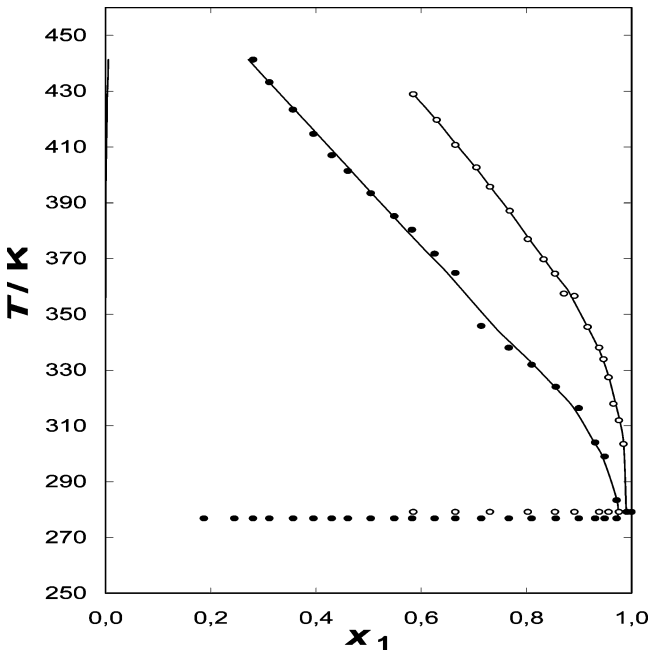

Figure 8. Solid−liquid and liquid−liquid phase equilibria of {C_2NTf_2 (1) + *n*-hexane, or *n*-octane (2)} binary systems: (●) *n*-hexane; (○) *n*-octane. Solid lines are calculated by means of the NRTL equation.

Information. As in all systems with ILs, the solubility of C_2NTf_2 in *n*-hexane is much lower than in benzene or dodecan-1-ol. The miscibility gap covers most of the mole fraction range of IL. The maximum of the solubility curve was at a low IL mole fraction, and the expected UCST was higher than 430 K. The results are shown in Figure 8.

The solid−liquid equilibrium of {C_2NTf_2 (1) + THF or DMSO (2)} binary systems have been also measured. The results are presented in Figures 9 and 10. A solid addition compound was observed with the empirical formulae: [$(C_2NTf_2)_3$·THF). It was a congruently melting compound at $T_{1,c}$ = 255.7 K and at composition $x_{1,c}$ = 0.75. From the DSC measurements for the mixture, the enthalpy of melting for this compound was found to be 480 J·mol^{-1}. Compound formation is attributed to strong O−H···O hydrogen bonds. We can also expect strong interaction between C_2NTf_2 and DMSO, because it is difficult to assume that the eutectic temperature will be as low as 150 K (obtained from the extrapolation of two liquidus curves). Unfortunately, it was impossible to measure this system at very low temperatures. The solidification of the mixture at temperatures lower than 240 K was noted.

Modeling. In addition to the experimental work, most of the IL/organic solvent systems were modeled using the general nonrandom two-liquid (NRTL) equation with linear temperature-

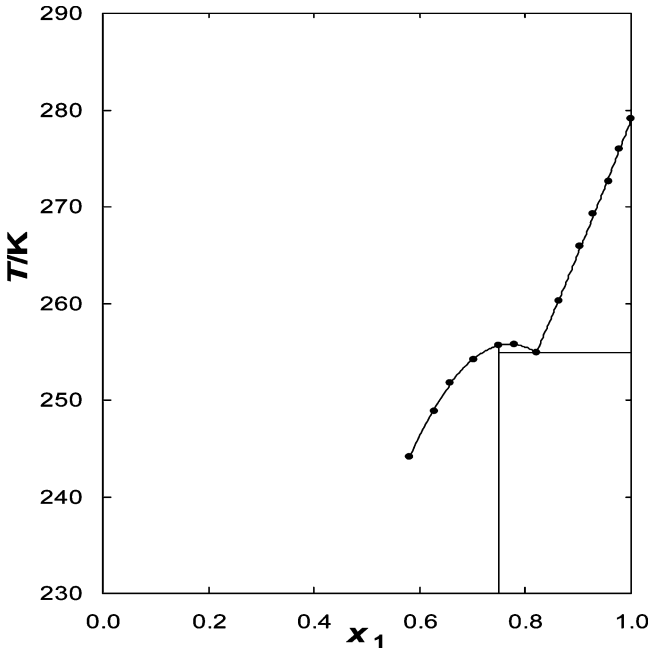

Figure 9. Solid−liquid phase equilibria of {C_2NTf_2 (1) + THF (2)} binary system; full lines drawn to guide the eye.

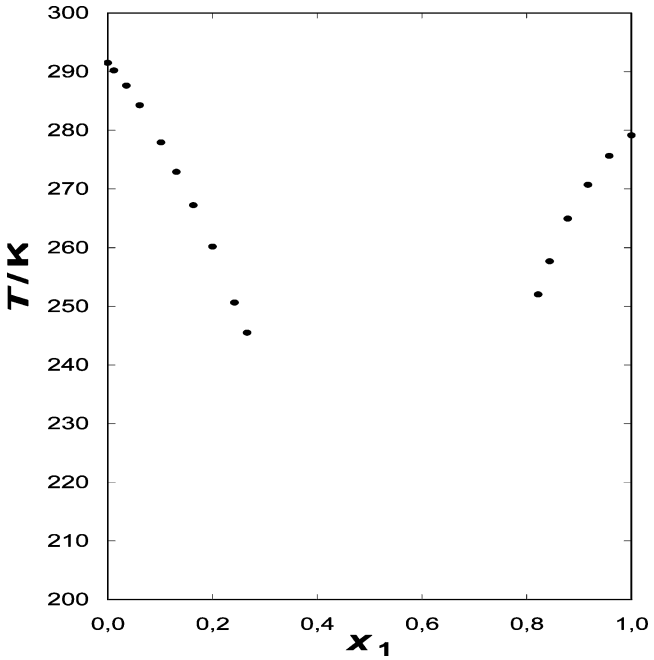

Figure 10. Solid−liquid phase equilibria of {C_2NTf_2 (1) + DMSO (2)} binary system.

dependent parameters. For solid−liquid equilibrium and liquid−liquid equilibrium, the same method and the same parameters were used to correlate the solute activity coefficients, γ_1, based on the NRTL model describing the excess Gibbs Energy[35]

$$\frac{G^E}{RT} = x_1 x_2 \left[\frac{\tau_{21} G_{21}}{x_1 + x_2 G_{21}} + \frac{\tau_{12} G_{12}}{G_{12} x_1 + x_2} \right] \quad (1)$$

$$\tau_{12} = (g_{12} - g_{22})/RT \quad (2)$$

$$\tau_{21} = (g_{21} - g_{11})/RT \quad (3)$$

$$G_{12} = \exp(-\alpha_{12}\tau_{12}) \quad (4)$$

$$G_{21} = \exp(-\alpha_{12}\tau_{21}) \quad (5)$$

$$\ln(\gamma_1) = x_2^2 \left[\tau_{21} \left(\frac{G_{21}}{x_1 + x_2 G_{21}} \right)^2 + \frac{\tau_{12} G_{12}}{(x_2 + x_1 G_{12})^2} \right] \quad (6)$$

The temperature-dependent model adjustable parameters ($g_{12} - g_{22} = a_{12} + b_{12}T$) and ($g_{21} - g_{11} = a_{21} + b_{21}T$) were found by minimization of the objective function OF:

$$\mathrm{OF} = \sum_{i=1}^{n} [(\Delta x_1)_i^2 + (\Delta x_1^*)_i^2] + \sum_{j=1}^{m} [(T_{\mathrm{exp},j} - T_{\mathrm{calc},j})^2] \quad (7)$$

where n is the number of experimental LLE points, m is the number of experimental SLE points, and Δx is defined as

$$\Delta x = x_{\mathrm{calc}} - x_{\mathrm{exp}} \quad (8)$$

The root-mean-square deviation of mole fraction was defined as follows:

$$\sigma_x = \left(\frac{\sum_{i=1}^{n} (\Delta x_1)_i^2 + \sum_{i=1}^{n} (\Delta x_1^*)_i^2}{2n - 2} \right)^{1/2} \quad (9)$$

where, x_1 is at ionic liquid rich phase and x_1* is at solvent rich phase. For every experimental LLE point, the values of x_1 and x_1* at constant temperature in the ionic liquid rich phase or solvent rich phase were described.

The solubility of a solid 1 in a liquid showing two solid−solid phase transitions before fusion may be expressed in a very general manner by eq 10. The solubility equation for temperatures below that of the phase transition must include the effect of the transition. The result for two first-order transitions is

$$-\ln x_1\gamma_1 = \frac{\Delta_{\mathrm{fus}}H_1}{R}\left(\frac{1}{T} - \frac{1}{T_{\mathrm{fus},1}}\right) + \frac{\Delta_{\mathrm{tr}}H_{1,\mathrm{I}}}{R}\left(\frac{1}{T} - \frac{1}{T_{\mathrm{tr},I}}\right) + \frac{\Delta_{\mathrm{tr}}H_{1,\mathrm{II}}}{R}\left(\frac{1}{T} - \frac{1}{T_{\mathrm{tr},II}}\right) - \frac{\Delta_{\mathrm{fus}}Cp_1}{R}\left(\ln\frac{T}{T_{\mathrm{fus},1}} + \frac{T_{\mathrm{fus},1}}{T} - 1\right) \quad (10)$$

where x_1, γ_1, $\Delta_{\mathrm{fus}}H_1$, $\Delta_{\mathrm{fus}}Cp_1$, $T_{\mathrm{fus},1}$, and T stand for mole fraction, activity coefficient, enthalpy of fusion, difference in solute heat capacity between the liquid and solid at the melting temperature, melting temperature of the ionic liquid (1), and equilibrium temperature, respectively. In this work, we did not measure $\Delta_{\mathrm{fus}}Cp_1$; thus, eq 10 was used without the last term.

The $\Delta_{\mathrm{tr}}H_{1,\mathrm{I}}$, $\Delta_{\mathrm{tr}}H_{1,\mathrm{II}}$, and $T_{\mathrm{tr,I}}$,$T_{\mathrm{tr,II}}$ stand for enthalpies of solid−solid transitions and transitions temperatures of the ionic liquid, respectively. Equation 10 is valid for simple eutectic mixtures with complete immiscibility in the solid phase. The root-mean-square deviation of temperature was defined as follows:

$$\sigma_T = \left[\sum_{j=1}^{m} \frac{(T_j^{\mathrm{calc}} - T_j^{\mathrm{exp}})^2}{n - 2} \right]^{0.5} \quad (11)$$

The model assumes that the anion and cation remain completely associated. Note that the UCST were not predicted from the fitting procedure since we did not expected an analytical mean field model like the NRTL equation, to adequately capture behavior near the critical point. The results shown in Figures 1−9 are typical of the NRTL modeling in this work and in many previously published.[20,21,30,32−34] The adjustable parameters with linear temperature dependence were vastly superior in reproducing the experimental phase equilib-

TABLE 3: Correlation of the SLE and LLE Data by Means of the NRTL Equation: Parameters ($g_{12}-g_{22}$) and ($g_{21}-g_{11}$) and Measures of Deviation σ_x and σ_T, (See Eqs 9 and 11)

	$g_{12}-g_{22}$/J·mol^{-1}		$g_{21}-g_{11}$/J·mol^{-1}				
solvent	a_{12}	b_{12}	a_{21}	b_{21}	α	σ_x	σ_T/K
water	−32968.91	144.81	−9726.54	58.33	0.40	0.0144	2.44
propan-1-ol	−38758.17	155.66	100763.23	−397.51	0.20	0.0003	
butan-1ol	−118447.80	709.45	−14115.64	78.40	0.20	0.0188	1.22
hexan-1-ol	−42124.64	180.57	54777.80	−149.16	0.35	0.0073	0.55
octan-1-ol	10834.21	−27.14	59184.62	−145.03	0.20	0.0028	
decan-1-ol	14591.32	−31.88	29205.59	−47.66	0.20	0.0042	
benzene	5221.31	−35.25	3318.89	54.77	0.20	0.0051	
toluene	−9532.93	51.69	−5375.90	98.65	0.30	0.0028	2.17
n-hexane	33044.65	−94.75	24944.87	4.42	0.20	0.0070	
n-octane	38906.96	−98.33	55186.11	−63.99	0.20	0.0018	

rium data than the temperature-independent parameters (not presented here), as was observed previously for the pirydynium ILs.[30] For the correlation of LLE, two points of equilibrium at the same temperature were described: the mole fraction of IL at IL rich phase and mole fraction of IL at solvent rich phase for every LLE equilibrium point from Tables 2 and 1S.

In this work, the value of parameter α (α = 0.2, α = 0.3, α = 0.35, or α = 0.4), a constant of proportionality similar to the nonrandomness constant of the NRTL equation, was used in the calculations for different binary systems.

Values of model parameters obtained by fitting solubility curves together with the corresponding standard deviations are given in Table 3. For systems presented in this work, the description of solid−liquid phase equilibrium was given by the average standard mean deviation (σ_T) of 1.6 K. Unfortunately, only for few systems it was possible to correlate the LLE and SLE equilibrium curves with this simple model and the same parameters with the reasonable results (see deviations σ_x and σ_T in Table 3). The prediction of the UCSTs or the eutectic points in (C_2NTf_2 + benzene, or toluene) binary systems was not acceptable.

Positive and negative deviations from ideality were found. The differences from ideality were not significant in most of the systems. The values of activity coefficients in the saturated solution ranged from 0.5 to about 100 for different experimental points. The highest values of activity coefficients were calculated for the solvent rich phase. This was particularly true for the aromatic and aliphatic hydrocarbons.

Octan-1-ol/Water Partitioning. The partition coefficient is normally used to assess the potential bioaccumulation and the distribution pattern of drugs and pollutants. The results of IL solubilities in octan-1-ol and water (from the left LLE curve extrapolated to 298.15 K) have given the base for calculation of the partition coefficients of C_2NTf_2 in system octan-1-ol/water at 298.15 K.

The experimental results in mole fraction are $x_{IL}{}^0 = 0.023$ and $x_{IL}{}^w = 0.005$ at temperature 298.15 K. It is evident that the low aqueous solubility of octan-1-ol has a negligible influence on the aqueous solubility of IL ("solute free" $x^o{}_o = 0.015$).[36] On the other hand, the rather large amount of water presented in octan-1-ol phase ("solute free" $x^o{}_w = 0.29$),[37] changes considerably the IL solubility in octan-1-ol phase, even the simple linear dependence for binary "solute free" solvent was assumed. Corresponding values of the C_2NTf_2 solubilities in mutually saturated solvent as a molar concentration in water saturated with octan-1-ol (c_1^{o*}) and octan-1-ol saturated water (c_1^{w*}) are 0.175 and 0.255, respectively. As it is shown in Table 2S of Supporting Information, the solute partition coefficient, defined as $P = c_1^{o*}/c_1^{w*}$, of C_2NTf_2 is less than one (0.68). The density of C_2NTf_2 at 298.15 K, measured for this calculation, is 1.4974 g·cm^{-3}. Indeed, the octan-1-ol/water partition coefficient for imidazolium salts, the log P were negative.[9,38] It is important to determine log P for such solutes to understand their behavior in the environment.

Concluding Remarks

We have presented a rapid and easy method of synthesis of ethyl(2-hydroxyethyl)dimethyl-ammonium bis(trifluomethylsulfonyl)imide. This low-temperature melting compound could be used for the phase transfer catalyst, as the additive to new processes as for extraction-separation processes,[41] for large-scale electroplating, as a substance enhancing lubrication for the motor oils, or as an anti-corrosive additive. Because of its solubility in water and short chain alcohols (this is a result of the interaction of the hydroxyl group at a side chain of cation and of polar anion), it should be tested as a possible wood preservative.

The phenomenon of two solid−solid phase transitions for C_2NTf_2 ionic liquid has been observed from DSC measurements. Solid−solid phase transition as a result of the changing structure of a solid phase at constant temperature and pressure is widely used in the energy storage. Unfortunately, in this case, the structures of the obtained salts were not described because the crystallization process is very complicated and also did not result in a monocrystal.

The applied salt has been surprisingly soluble in benzene. The immiscibility gap in the liquid phase was at low mole fraction of IL, but the UCST was at high temperature (>430 K). The phase diagram of ILs with benzene and benzene derivatives differ from those with aliphatic hydrocarbons. The solubility of ILs is much higher in aromatic hydrocarbons than in aliphatic hydrocarbons and cyclohydrocarbons, because of the interaction with the benzene ring. The interaction between the IL and benzene can be sometimes very strong forming well-organized phases as clatrate-type structures in the liquid phase.[42] In our work, the strong interaction was observed for the IL with THF and DMSO, which in the case of THF resulted in a congruently melting compound at low temperature.

The solid−liquid phase diagrams have shown simple eutectic mixtures. The results of the correlation of SLE and LLE were acceptable with the NRTL equation using linear temperature dependence parameters.

The logarithm of octan-1-ol/water partition coefficient is negative, as it was observed for 1,3-dialkilimidazolium chlorides, alkyl(2-hydroxyethyl)dimethylammonium bromides, and many other ILs.[9,38] Compared to conventional organic substances, the IL investigated here is polar and is capable of undergoing many types of interactions.

Acknowledgment. This work was supported by the Warsaw University of Technology under Project of the University

Scientific Program, UPB 2007. Authors would like to thank Dr. R. Bogel-Łukasik for the synthesis of ammonium salt.

Supporting Information Available: Nuclear magnetic resonance, DSC diagram, TG/DTA diagram, experimental SLE/LLE data, octan-1-ol/water partition coefficient. This information is available free of charge via the Internet at http://pubs.acs.org.

References and Notes

(1) Pernak, J.; Skrzypczak, A.; Lota, G.; Frąckowiak, E. *Chem. Eur. J.* **2007**, DOI: 10.1002/chem.200601243.
(2) Pernak, J.; Chwała, P.; Syguda, A. *Polish J. Chem*. **2004**, *78*, 539−546.
(3) Pernak, J.; Chwała, P. *Eur. J. Med. Chem*. **2003**, *38*, 1035−1042.
(4) Pernak, J.; Chwała, P.; Syguda, A.; Poźniak, R. *Polish J. Chem*. **2003**, *77*, 1263−1274.
(5) Mévellec, V.; Leger, B.; Mauduit, M.; Roucoux, A. *Chem. Commun*. **2005**, 2838−2839.
(6) Pernak, J.; Smiglak, M.; Griffin, S. T.; Hough, W. L.; Wilson, T. B.; Pernak, A.; Zabielska-Matejuk, J.; Fojutowski, A.; Kita K.; Rogers, R. D. *Green Chem.* **2006**, *8*, 798- 806.
(7) Domańska, U.; Bąkała, I.; Pernak, J. *J. Chem. Eng. Data* **2007**, *52*, 309−314.
(8) Domańska, U.; Ługowska, K.; Pernak, J. *J. Chem. Thermodyn*. **2007**, *39*, 729−736.
(9) Domańska, U.; Bogel-Łukasik, R. *J. Phys. Chem. B* **2005**, *109*, 12124−12132.
(10) Domańska, U.; Bogel-Łukasik, R. *Fluid Phase Equilib*. **2005**, *233*, 220−227.
(11) Domańska, U. *Thermochim. Acta* **2006**, *448*, 19−30.
(12) Pernak, J.; Feder-Kubis, J. *Chem. Eur. J*. **2005**, *11*, 4441−4449.
(13) Wasserscheid, P.; Keim, W. *Angew. Chem*. **2000**, *39*, 3772−3789.
(14) Dupont, J.; deSouza, R. F.; Suarez, P. A. Z. *Chem. Rev*. **2002**, *102*, 3667−3692.
(15) Enders, F.; El Abedin, S. Z. *Phys. Chem. Chem. Phys*. **2006**, *8*, 2101−2116.
(16) Chappe, C.; Pieraccini, D. *J. Phys. Org. Chem*. **2005**, ***18***, 275−297.
(17) Belvèze, L. S.; Brennecke, J. F.; Stadtherr, M. A. *Ind. Eng. Chem. Res*. **2004**, *43*, 815−825.
(18) Domańska, U. *Pure Appl. Chem*. **2005**, *77*, 543−557.
(19) Marsh, K. N.; Deev, A.; Wu, C.-T.; Tran, E.; Klamt, A. *Korean J. Chem. Eng*. **2002**, *19*, 357−362.
(20) Domańska, U.; Marciniak, A. *J. Phys. Chem. B* **2004**, *108*, 2376−2382.
(21) Domańska, U.; Marciniak, A. *Fluid Phase Equilib.* **2007**, *260*, 9−18.
(22) Domańska, U.; Marciniak, A. *Green Chem*. **2007**, *9*, 262−266.
(23) Domańska, U.; Pobudkowska, A.; Eckert, F. *J. Chem. Thermodyn*. **2006**, *38*, 685−695.
(24) Wu, C. T.; Marsh, K. N.; Deev, A. V.; Boxall, J. A. *J. Chem. Eng. Data* **2003**, *48*, 486−491.
(25) Sahandzhieva, K.; Tuma, D.; Breyer, S.; Kamps, P.-S.; Maurer, G. *J. Chem. Eng. Data* **2006**, *51*, 1516−1525.
(26) Heintz, A.; Lehman, J. K.; Wertz, Ch. *J. Chem. Eng. Data* **2003**, *48*, 472−474.
(27) Crosthwaite, J. M.; Akai, S. V. K.; Maginn, E. J.; Brennecke, J. B. *Fluid Phase Equilib.* **2005**, *228*−*229*, 303−309.
(28) Crosthwaite, J. M.; Maginn, E. J.; Brennecke, J. B. *J. Phys Chem. B* **2004**, *108*, 5113−5119.
(29) Najdanovic-Visak, V.; Esperanca, J. M. S. S.; Rebelo, L. P. N.; Nunes da Ponte, M.; Guedes, H. J. R.; Seddon, K. R.; De Sousa, H. C.; Szydłowski, J. *J. Phys. Chem. B* **2003**, *107*, 12797−12807.
(30) Crosthwaite, J. M.; Muldoon, M. J.; Akai, S. V. K.; Maginn, E. J.; Brennecke, J. B. *J. Phys. Chem. B* **2006**, *110*, 9354−9361.
(31) Domańska, U.; Casás, L. *J. Phys. Chem. B* **2007**, *111*, 4109−4115.
(32) Domańska, U.; Pobudkowska, A.; Eckert, F. *Green Chem*. **2006**, *8*, 268−276.
(33) Domańska, U.; Marciniak, A. *J. Chem. Thermodyn*. **2005**, *37*, 577−585.
(34) Domańska, U.; Marciniak, A. *J. Chem. Eng. Data* **2003**, *48*, 451−456.
(35) Renon, H.; Prausnitz, J. M. *AIChE J*. **1968**, *14*, 135−144.
(36) Domańska, U.; Kozłowska, M. K.; Rogalski, M. *J. Chem. Eng. Data* **2002**, *47*, 456−466.
(37) Dallas, A. J.; Carr, P. W. *J. Chem. Soc., Perkin Trans*. **1992**, *2*, 2155−2160.
(38) Ropel, L.; Belvéze, L. S.; Akai, S. V. K.; Stadtherr, M. A.; Brennecke, J. F. *Green Chem*. **2005**, *7*, 83−90.
(39) Diaz-Pena, M.; Tardajos, G. *J. Chem. Thermodyn*. **1979**, *11*, 441−445.
(40) Steckel, F.; Szapiro, S. *Trans. Faraday Soc*. **1963**, *59*, 331−343.
(41) Domańska, U.; Pobudkowska, A.; Królikowski, M. *Fluid Phase Equilib*. **2007**, *259*, 173−179.
(42) Łachwa, J.; Bento, I.; Duarte, M. T.; Lopes, J. N. C.; Rebelo, L. P. N. *Chem. Commun*. **2006**, 2445−2447.